# Translocation of $AT_1$- and $AT_2$-Receptors by Higher Concentrations of Angiotensin II in the Smooth Muscle Cells of Rat Internal Anal Sphincter

**Márcio A. F. de Godoy and Satish Rattan**

*Department of Medicine, Division of Gastroenterology & Hepatology, Jefferson Medical College of Thomas Jefferson University, Philadelphia, PA (MAFDG and SR)*

**Running Title:** Cellular trafficking of Ang II receptors

[1]**Corresponding Author:** Dr. Satish Rattan, Jefferson Medical College, Thomas Jefferson University, 1025 Walnut Street, Room # 901 College; Philadelphia, PA 19107

Tel # (215) 955-5614; Fax # (215) 503-3771; Email: Satish.Rattan@Jefferson.edu

**Number of text pages:** 19

**Number of tables:** 2

**Figures:** 7

**References:** 25

**Number of words in abstract:** 220

**Number of words in introduction:** 504

**Number of words in discussion:** 845

**Abbreviations:** Ang II, angiotensin II; $AT_1$-R, angiotensin receptor/s subtype I; $AT_2$-R, angiotensin receptor/s subtype II; IAS, internal anal sphincter; IOD, integrated optical density; IR, immunoreactivity; NCM, nitrocellulose membrane; PM, plasma membrane; RT-PCR, reverse transcriptase-polymerase chain reaction; KPS, Krebs' physiological solution; RT, room temperature; SMC, smooth muscle cell, FITC, fluorescein isothiocyanate; TR, Texas red; PD123,319, [*S*-(+)-1-([4-(dimethylamino)-3-methylphenyl]methyl)-5-(diphenylacetyl)-4,5,6,7-tetrahydro-1*H*-imidazo(4,5-*c*)pyridine-6-carboxylic acid] ($AT_2$-R antagonist).

**Recommended section:** Gastrointestinal, Hepatic, Pulmonary, & Renal

## Abstract

Previous studies have reported bimodal effects by Ang II in the rat internal anal sphincter (IAS), a concentration-dependent contraction (at lower concentrations) and relaxation (at higher concentrations). The experiments suggest the above responses are the result of Ang II subtype I receptor/s ($AT_1$-R) and subtype II receptor/s ($AT_2$-R) activation, respectively. These studies determined the role and mechanism of $AT_2$-R-induced relaxation of the smooth muscle cells (SMC) from the IAS in response to Ang II. Laser confocal microscopy showed that in the basal state the $AT_1$-R reside in the plasma membrane while $AT_2$-Rs are present in the cytosol. Higher concentrations of Ang II caused movement of $AT_1$-R and $AT_2$-R in opposite directions to the cytosol and the membrane, respectively. Losartan ($AT_1$-R antagonist) but not PD123,319 ($AT_2$-R antagonist) selectively inhibited these movements. These results are based on biotinylation assays, confocal images, and Western blot analyses of the $AT_1$-Rs and $AT_2$-Rs densities in the plasma membrane vs. cytosolic fractions of the IAS SMC. Ang II in higher concentrations did not change the total contents of Ang II receptors. These data combined with the functional data using measurements of IAS SMC lengths suggest that internalization of $AT_1$-R and externalization of $AT_2$-R may be responsible for the activation of the $AT_2$-R, which leads to the relaxation of the IAS with higher concentrations of Ang II.

JPET Fast Forward. Published on September 19, 2006 as DOI: 10.1124/jpet.106.108084
This article has not been copyedited and formatted. The final version may differ from this version.



## Introduction

Angiotensin II (Ang II) has been implicated in a wide range of physiological processes by the activation of specific membrane receptors in the target cells. Ang II binds to two different subtypes of G-protein-coupled receptors, $AT_1$ ($AT_1$-R) and $AT_2$ ($AT_2$-R) (De Gasparo et al., 2000). For several years, most of the effects of Ang II were attributed to the activation of the $AT_1$-R subtype. Recently, however, an increasing number of reports also suggested the involvement of $AT_2$-R in the actions of Ang II (Siragy et al., 2000; Rattan et al., 2002; Wu et al., 2001; De Godoy and De Oliveira, 2002; De Godoy et al., 2004b).

Internal anal sphincter (IAS) studies in rats suggested that locally generated Ang II contributes in part to the basal tone in the IAS (De Godoy et al., 2004b). A multipronged approach of functional, biochemical, and molecular biology showed the expression of angiotensinogen, renin, and ACE in the IAS at the gene and protein levels (De Godoy and Rattan, 2005). More recently, we showed the presence of the highest levels of renin-angiotensin system components, Ang II and $AT_1$-R to be in the tonic IAS vs. the adjoining phasic smooth muscles of the rectum and anococcygeus (De Godoy and Rattan, 2005).

Although Ang II contracts the IAS via activation of $AT_1$-Rs, there is a physiological brake for this effect. In the rat IAS Ang II produces bimodal effect, a contraction (at lower concentrations) followed by relaxation (at higher concentrations). Experiments with selective antagonists (losartan for $AT_1$-R and PD123,319 for $AT_2$-R) further show that contractions are mediated by $AT_1$-R and relaxation is mediated by $AT_2$-R (De Godoy et al., 2004b). The bimodal effect of Ang II may be explained on the basis of either differences in the receptor affinity for $AT_1$-R vs. $AT_2$-R or in the receptor trafficking between the cytosol and the plasma membrane (PM). The first possibility is less likely because of the similar affinity for both subtypes of receptors (De Gasparo et al., 2000). Present studies focus on the hypothesis that once externalized to the membrane $AT_2$-Rs exert their inhibitory effect on the IAS smooth muscle cells (SMC).

Using different systems, it was shown before that short exposures to high concentrations of Ang II lead to internalization of $AT_1$-R (Hein et al., 1997; Olivares-Reyes et al., 2001). We hypothesize here that the internalization of $AT_1$-R with similar exposures of Ang II may release $AT_2$-R from the state of

inactivity, causing relaxation of the smooth muscle. To test this hypothesis, we used laser confocal microscopy and biotinylation to determine the location of $AT_1$- and $AT_2$-R in the SMC isolated from rat IAS. We also used Western blot analysis to investigate the relative distribution of $AT_1$- and $AT_2$-R in the particulate vs. cytosolic fractions of the SMC. Our data show that high concentrations of Ang II cause $AT_1$-R internalization and externalization of $AT_2$-R to the PM. The opposite trafficking of $AT_1$- and $AT_2$-R may be partly responsible for the relaxation in response to the higher concentrations of Ang II.

## Materials and Methods

**Isolation of Smooth Muscle Cells (SMC), and Measurement of Cell Length.** Male Sprague-Dawley rats (300-350 g) were sacrificed by decapitation and the IAS smooth muscle strips were prepared as described before (De Godoy et al., 2004b; De Godoy et al., 2004a). The circular IAS smooth muscle strips (~ 0.5 mm x 7 mm) were prepared in oxygenated Krebs' physiological solution (KPS). The composition of KPS was as follows (in mM): 118.07 NaCl, 4.69 KCl, 2.52 $CaCl_2$, 1.16 $MgSO_4$, 1.01 $NaH_2PO_4$, 25 $NaHCO_3$, and 11.10 glucose. The experimental protocol of the study was approved by the Institutional Animal Care and Use Committee of Thomas Jefferson University and was in accordance with the recommendations of the American Association for the Accreditation of Laboratory Animal Care.

SMCs from IAS were isolated as described previously (Rattan et al., 2002; Cao et al., 2002; Huang et al., 2005; Rattan and Chakder, 1992). Briefly, IAS was cut into small pieces (~1 mm cubes), and incubated in oxygenated KPS containing 0.1% collagenase and 0.01% soybean trypsin inhibitor at 37°C for two successive 1 h periods. The mixture was then filtered through a 500 μm Nitex mesh. The tissue trapped on the mesh was rinsed with 25 ml (5 × 5 ml) collagenase-free KPS. The tissue was incubated in collagenase-free KPS at 37°C, and dispersion of the cells (0-1 h) was monitored periodically by examining a 10-μl aliquot of the mixture microscopically. The SMCs were then harvested by filtration through the Nitex mesh. The filtrate containing the cells was centrifuged at 350g for 10 min at room temperature (RT). The cells in the pellet were re-suspended in oxygenated KPS (at 37ºC) at a cell density of $3 \times 10^4$ cells/ml.

Individual cell lengths were measured by micrometry using phase contrast microscopy on a custom-assembled microscope (Olympus, Tokyo, Japan), close-circuit video camera (model Pulnix MC-7; PULNIX America, Inc., Sunnyvale, CA), and PC computer. Digital images of the cells were stored and the cell lengths measured by the Image-Pro Plus version 4.0 program (Media Cybernetics, Silver Spring, MD).

Following exposure with Ang II (0.1 nM to 10 μM) for 10 min, the SMCs were fixed with acrolein (final concentration 1%) and transferred onto chrome-alum coated glass slides (Fisher Scientific, Pittsburg, PA). The studies were repeated in the presence of selective antagonists (losartan for $AT_1$-R and PD123,319 for $AT_2$-R, both at 100 nM). The shortening of SMC in each category of experiments was calculated on the bases of the original cell lengths. The studies were repeated in the SMC isolated from at least three animals.

**Receptor Internalization Assay**. To determine the time-course effect of high concentrations of Ang II on the cellular localization of $AT_1$- and $AT_2$-R in the IAS SMC, freshly isolated cells from the IAS were resuspended in DMEM medium containing 10 μM amastatin. Cells were aliquoted in groups and exposed to 1 nM to 10 μM Ang II for 0 to 30 min intervals in 5% $CO_2$ humidified atmosphere at 37ºC. Another group of cells was exposed to 100 μM bethanechol for 30 min. The cells were then biotinylated on ice in a rocking platform with 0.5 mg/ml Sulfo-NHS-SS-biotin (Pierce, Rockford, IL) for 30 min as previously described (Huang et al., 1999). The cells were then centrifuged at 1,000 g and lysed immediately for protein extraction. Biotinylated proteins were affinity-purified from cell lysate with streptavidin-agarose (Invitrogen Corporation, Carlsbad, CA) and loaded onto a sodium dodecyl sulfate (SDS) – 10% of polyacrilamide gel. Western blot was then performed as described below.

**Immunofluorescence and Confocal Microscopy.** SMCs were isolated as described above and incubated in a culture medium containing 10 μM amastatin (to inhibit Ang II degradation) for 10 min in the absence or presence of Ang II (100 nM to 10 μM). Experiments were repeated in the presence of losartan or PD123,319 (100 nM) previously incubated for 20 min. Immunocytochemistry of the SMC

was performed by indirect immunofluorescence as described before (Battish et al., 2000). SMCs were fixed with ice-cold fixative (4% paraformaldehyde and 0.2% picric acid in PBS, pH 7.4) for 10 min and then thoroughly washed in PBS. The cells were then rinsed with PBS and incubated in a mixture of 1:200 primary antibody ($AT_1$ raised in rabbit and $AT_2$ raised in goat) and then diluted in PBS containing 0.5% BSA, and 0.2% Triton X-100 overnight at RT in a humid chamber. Cells were then rinsed with PBS and incubated in a mixture of Texas red (TR) and FITC-labeled secondary antibodies (1:200 in a solution of 2% normal donkey serum and 0.3% Triton X-100 in PBS) raised in donkey against rabbit and goat immunoglobulins respectively.

The slides containing the cells were incubated for 60 min at RT, rinsed with PBS, air dried, and cover slipped with Vectashield (Vector Labs, Burlingame, CA). Cells were examined using a Confocal Laser Scanning Microscope System interfaced to a Zeiss Axiovert 200 M inverted microscope (Carl Zeiss Microimaging, Inc., Thornwood, NY) at the Kimel Cancer Center's Bioimaging Facility of our institution. The plot profile of the pixel intensities (gray scale: 0 to 250) was analyzed as described previously (Chiba et al., 2004). Briefly, using Image-Pro Plus 4.0, the pixel intensities over the outer 15% of each cell width were taken as an index of peripheral AT-R, whereas those over the remaining central 70% of the cell width were estimated as cytosolic AT-R. The average peripheral to cytosolic ratio of 2 lines scans in each cell was calculated by dividing the gray value of the highest peak at 15% by the highest peak at 70%. Six randomly selected cells were analyzed for each experimental condition.

**Western Blot Analysis.** SMCs were treated with Ang II (1 nM to 10 μM) for 10 min as described above. Western blot analyses were performed to determine the relative distribution of $AT_1$- and $AT_2$-R following the approach previously described (Rattan et al., 2002). Briefly, the SMC were homogenized in lysis buffer (10 mM Tris-HCl, pH 7.5, 5 mM MgCl2, 2 mM EDTA, 250 mM sucrose, 1 mM dithiothreitol, and 1 mM sodium orthovanadate), centrifuged for 10 min at 100,000 g at 4ºC (Beckman, Fullerton, CA; Optima TLX Ultracentrifuge), and the supernatant was collected as the cytosolic fraction. The precipitate (the particulate or membrane fraction) was dissolved in 1% sodium dodecyl sulfate (SDS)-containing lysis buffer and the respective protein contents determined by the method of Lowry et

JPET Fast Forward. Published on September 19, 2006 as DOI: 10.1124/jpet.106.108084
This article has not been copyedited and formatted. The final version may differ from this version.



al. (Lowry et al., 1951). The proteins were then separated by Gel electrophoresis followed by their transfer to the nitrocellulose membrane (NCM) by electrophoresis at 4°C.

The NCM was then incubated with the specific primary antibodies (rabbit IgG, 1:500) for 2 h at RT. After washing with TBS-T, the NCMs were incubated with HRP labeled-secondary antibody (1:10,000) for 1 h at RT. The corresponding bands were visualized with enhanced chemiluminescence substrate using the SuperSignal® West Pico Chemiluminescent Substrate (Pierce, Rockford, IL) and Hyperfilm MP (Amersham Bioscience, Corp., NJ).

NCMs were then stripped of antibodies using Restore™ Western Blot Stripping Buffer (Pierce, Rockford, IL) for 15 min at RT. NCMs were reprobed for α-actin using the specific primary (mouse IgG 1:10,000 for α-actin) and secondary (1:10,000) antibodies. Bands of interest were scanned (SnapSacn.310; Agfa, Ridgefield Park, NJ) and the respective areas and integrated optical density (IOD) were determined using Image-Pro Plus 4.0. The relative densities were calculated by normalizing the IOD of each blot with that of α-actin.

**RT-PCR**. IAS SMCs were exposed to 10 μM Ang II for 10 min. Total RNA was isolated and purified by the acid guanidine-phenol-chloroform method (Chomczynski and Sacchi, 1987) and quantified by measurement of absorbance at 260 nm in a spectrophotometer. Total RNA (2 μg) was subjected to first-strand cDNA synthesis using oligo dT primers (Promega, Madison, WI) and Omniscript RT Kit (Qiagen, Germantown, MD) in a final volume of 20 μl at 42°C for 60 min. PCR primers specific for $AT_1$-R, $AT_2$-R, and β-actin cDNA were designed as shown in Table 1. PCR was performed in a Promega 2x Master Mix (M750B, Promega, Madison, WI) in a final volume of 25 μl, using a Perkin-Elmer Thermal Cycler (PerkinElmer Life and Analytical Sciences, Inc., MA). The PCR conditions consisted of 94°C for 5 min (for the initial denaturation phase) followed by 35 cycles of 94°C for 30s (denaturation), 57°C for 30s (annealing), and 72°C for 1 min (extension), with a final extension at 72°C for 7 min. The PCR products were separated on 1.5% (w/v) agarose gel containing ethidium bromide and

were visualized with UV light. The relative densities were calculated by normalizing the IOD of each blot with that of β-actin.

**Data Analysis.** Results were expressed as means ± S.E.M. Concentration-response curves were analyzed using a non-linear interactive fitting program (GraphPad Prism 3.0, Graph Pad Software Incorporated, CA). Agonist potencies and maximum responses were expressed as $pD_2$ (negative logarithm of the molar concentration of agonist producing 50% of the maximum response) and $E_{max}$ (maximum effect elicited by the agonist), respectively, calculated from the concentration-response curves. Biotinylation data for $AT_1$- and $AT_2$-R were expressed on the basis of their respective % maximal IOD at the cell surface. Statistical significance was tested by the one-way analysis of variance (ANOVA) followed by the Dunnett post-hoc test when three or more different groups were compared. The unpaired student t-test was used to compare only two different groups. A 'p' value less than 0.05 was considered to be statistically significant.

**Drugs and Antibodies.** Ang II, amastatin, and PD123,319 were from Sigma-Aldrich (St. Louis, MO). Losartan was a gift from Merck (Rahway, NJ). All antibodies were from Santa Cruz Biotechnology, Inc. (Santa Cruz, CA). All PCR primers were from MWG (MWG-Biotech Inc., High Point, NC).

## Results

**Effect of Ang II on SMC Length.** IAS SMCs were suspended in oxygenated KPS at 37ºC. The cells next were exposed to different concentrations of Ang II (0.1 nM to 10 μM) for 10 min. Results showed contractions in the lower range of concentrations (0.1 nM to 100 nM) and relaxation in the higher concentrations (1-10 μM). The largest decrease was at 10 μM Ang II and, therefore, was the concentration used in the subsequent experiments (Fig. 1). Incubation with losartan (100 nM) significantly (*; $p < 0.05$) inhibited the contractile phase of Ang II response. On the other hand, PD123,319 significantly (*; $p < 0.05$) inhibited the relaxation component, without any significant effect

JPET Fast Forward. Published on September 19, 2006 as DOI: 10.1124/jpet.106.108084
This article has not been copyedited and formatted. The final version may differ from this version.



on the contractile phase (*; $p > 0.05$). These data suggest that the bimodal effect by Ang II in the IAS SMCs is because of the activation of $AT_1$-Rs in the contractile phase and the activation of the $AT_2$-Rs in the relaxation phase. Data for $E_{max}$ and $pD_2$ values are provided in table 2.

**Effect of Ang II (10 μM) on AT1-R Internalization using Biotinylation.** For the quantitation of the cell surface population of Ang II receptors, we performed biotinylation assays following a time course (0 to 30 min) after pretreatment of the cells with 10 μM Ang II. The IAS SMCs were isolated, biotinylated with Sulfo-NHS-SS-biotin, and lysed for protein extraction. Biotinylated proteins were purified by the streptavidin-agarose method, and $AT_1$-R (Fig. 2A) and $AT_2$-R (Fig. 2B) were monitored by Western blot analysis followed by densitometry analysis. Ang II (10 μM) produced a significant decrease in $AT_1$-R (suggesting internalization) or increase in $AT_2$-R (suggesting externalization) at the IAS SMC surface, in a time-dependent manner that plateaued at 10 min (*; $p < 0.05$; Fig. 2C). Bethanechol (100 μM) produced no significant change in the density of Ang II receptors on the cell surface (data not shown).

**Internalization of $AT_1$-R Examined by Confocal Microscopy.** Confocal microscopy was used to determine the localization of $AT_1$-Rs in IAS SMCs after treatment with 10 μM Ang II for 10 min. IAS SMCs were isolated, fixed and exposed to primary antibodies for Ang II receptors and to secondary antibodies marked with TR (for $AT_1$-Rs) or FITC (for $AT_2$-Rs). Semi-quantitative analyses of the confocal images were performed by the plot profile of the pixel intensities over the 15% of each cell width (taken as the periphery) and over those in the remaining 70% width (taken as cytosolic) to further support these data. The results are expressed as the average peripheral to cytosolic ratio of line scans. Strong IR for $AT_1$-R was found in the PM and in the cytosolic perinuclear area (Fig. 3a) of cells in the basal state. Incubation with Ang II (100 nM to 10 μM) decreased the $AT_1$-R-IR in the PM and increased it in the cytosol (Figs. 3b and 3c). Losartan alone produced a significant increase of $AT_1$-R-IR in the PM (Fig. 3d) and competitively inhibited the internalization of $AT_1$-Rs (Figs. 3e and 3f). PD123,319 produced no significant effect on the cellular distribution of $AT_1$-R under any of the conditions tested

(Figs. 3g, 3h, and 3i). The semi-quantitative analyses show $AT_1$-R trafficking from PM to cytosol by the higher concentration of Ang II (Fig. 3B).

By contrast with the $AT_1$-R, most of the $AT_2$-R-IR were found to be distributed evenly in the cytosol of the IAS SMC (Fig. 4a). Higher concentrations of Ang II increased the $AT_2$-R-IR in the PM while almost eliminating them from the cytosol (Figs. 4b and 4c). Losartan produced no significant effect in the basal state (Fig. 4d) but inhibited $AT_2$-R migration to PM (Figs. 4e and 4f). PD123,319 produced no significant effect under any of the conditions tested (Figs. 4g, 4h, and 4i). The semi-quantitation analysis by plot profile revealed trafficking of $AT_2$-Rs from cytosol to PM by Ang II (Fig. 4B).

**Relative Distribution of $AT_1$-R in the Particulate vs. Cytosolic Fractions of the IAS SMC.** The effects of Ang II on the relative distribution of Ang II receptors in the PM and in the cytosol of IAS SMCs were evaluated by Western blot. After exposure to different concentrations of Ang II (1 nM to 10 μM) in oxygenated KPS at 37ºC for 10 min, the total cellular protein was extracted and the cytosolic and PM fractions separated by a high speed centrifuge as described above. Proteins were then separated by gel electrophoresis and blotted by chemiluminescence. The resulting bands were identified by their molecular weight and the relative density analyzed by densitometry on the gray scale. The typical bands for $AT_1$-R were at 43 to 56 kDa. In the basal state, the relative density of $AT_1$-Rs was higher in the particulate fraction of IAS SMC. Ang II caused a concentration-dependent decrease in $AT_1$-R density in the particulate fraction but caused an increase in the cytosolic fraction (Fig. 5A).

**Relative Distribution of $AT_2$-R in the Particulate vs. Cytosolic Fractions of the IAS SMC Extracts.** The typical bands for $AT_2$-R expression were at 50 to 70 kDa. The relative density of $AT_2$-R was higher in the cytosolic as compared with the particulate fraction in the basal state. Higher concentration of Ang II caused a significant decrease in the $AT_2$-R density in the cytosolic fraction (Fig. 5B) without a significant change in the density of 50 to 70 kDa $AT_2$-R in the particulate fraction. However, there was a significant increase in the density of 105 to 120 kDa $AT_2$-R. The latter represents a homodimer of $AT_2$-R (two units physically bound) as has already been shown in previous studies in different systems (Lazard et al., 1994).

**Effects of Ang II on $AT_2$ and $AT_1$ Expression.** We evaluated the effects of Ang II in the overall transcriptional and translational expression of $AT_1$-R and $AT_2$-R in the total cell extracts using RT-PCR and Western blot analyses after exposure to 10 μM Ang II for 10 min. Western blot analysis revealed no significant change in the expression of either $AT_1$-R or $AT_2$-R following the pretreatment with Ang II ($p > 0.05$; $n = 3$; Figs. 6A and 6B).

These results were confirmed by the transcriptional expression via RT-PCR ($p > 0.05$; $n = 3$; Figs. 7A and 7B). Longer incubation times (up to 180 min) did not produce any significant change in the transcriptional and translational expression of $AT_1$-Rs and $AT_2$-Rs (data not shown).

## Discussion

Bimodal effect of Ang II (contraction with the lower concentrations and relaxation with the higher) in different smooth muscle tissues including the IAS (De Godoy et al., 2004b; De Godoy et al., 2004a; Fukada et al., 2005) has been known for some time. These studies provide a mechanism for that bimodal effect of Ang II in the IAS smooth muscle using functional and molecular approaches in the isolated SMC.

Functional studies in the IAS SMC show that concentrations of Ang II lower than 100 nM induce contraction, while higher concentrations produce relaxation (Fig. 1). These results in the isolated SMC are conceptually similar to those obtained in the intact IAS smooth muscle strips (De Godoy et al., 2004b), except for quantitative differences in the amplitude of the responses. This may be because of differences in the responses of the IAS SMC when they are *in situ* conditions of basal tone (for the smooth muscle strips experiments) as compared with when they are examined under isolated conditions (as is the case in the present studies). In support of that concept, chemo-mechanical studies in the arterial SMC (Yang et al., 2003) have shown that the absence of tension imbalances the electrolyte behavior, protein phosphorylation, and protein-protein interactions in the SMCs.

Ang II has a similar affinity for both $AT_1$-R and $AT_2$-R (De Gasparo et al., 2000). Experiments with the selective antagonists (losartan for $AT_1$-R, and PD123,319 for $AT_2$-R) show that activation of $AT_1$-R induces contractions and activation of $AT_2$-R produces relaxation of the IAS SMCs. Lack of overlapping

effects of the antagonists suggests that the $AT_1$-R are activated in the lower concentrations, and that $AT_2$-R, on the other hand, are activated at the higher ranges of Ang II concentrations.

Quantitative determination of $AT_1$- and $AT_2$-R in the PM via biotinylation studies after different exposure times with 10 μM Ang II ($E_{max}$ concentration) show that migration of $AT_1$-Rs from the PM while those of $AT_2$-Rs to the PM plateau at 10 min (Fig. 2). Confocal microscopy studies confirm these findings (Figs. 3 and 4). Losartan, but not PD123,319 (Figs. 3B and 4B), inhibits this what suggests that $AT_1$-R activation causes the trafficking of $AT_1$- and $AT_2$-R in the opposite direction. Losartan by itself produces a significant increase in the $AT_1$-R density on the PM of IAS SMCs, suggesting that inactivation of $AT_1$-R prevents constitutive internalization of the receptor.

As discussed above, a major mechanism for the switch from $AT_1$- to $AT_2$-R activation is the activation of $AT_1$-R. In addition, reports show that Ang II receptor trafficking and desensitization depend on β-arrestin recruitment (Turu et al., 2006) and on G protein-coupled receptor kinases activities such as the G protein-coupled kinase-5 and the beta adrenoceptor kinase 1 (Rockman et al., 1996; Kim et al., 2005). The specific role of G-protein-coupling in the switch from $AT_1$- to $AT_2$-R in the IAS smooth muscle remains to be identified. However, this switch appears to be specific to $AT_1$-R activation because bethanechol (a muscarinic agonist that also produces smooth muscle contraction via the activation Gq-couple signaling) does not modify the cellular distribution of $AT_1$- and $AT_2$-R in the IAS SMC.

Western blot experiments confirm Ang II concentration-dependence for the trafficking of Ang II receptor subtypes. The higher concentrations of Ang II cause the movement of $AT_1$-R from the PM to the cytosol (Fig. 5A), while reverse is the case for $AT_2$-R. Higher concentrations of Ang II decrease the density of $AT_2$-R in the cytosolic fraction (Fig. 5B) and promote its migration towards the periphery of the SMC. Our studies demonstrate specific increase in the relative density of 105 to 120 kDa bands for $AT_2$-R in the particulate fraction of the SMC with high concentrations of Ang II. In agreement with this concept, earlier studies in the human myometrium SMC have reported a similar increase in $AT_2$-R homodimers in the PM (Lazard et al., 1994). RT-PCR analyses further show that relaxation of the SMC with higher concentrations of Ang II is associated with the cross-translocation of $AT_1$-R and $AT_2$-R rather

than an overall change in their population density (Figs. 7). In addition, our preliminary studies suggest that short exposure (10 min) of higher concentration of Ang II are appropriate for the changes in $AT_1$- and $AT_2$-R trafficking since there was no significant difference in this trafficking pattern when the cells are exposed to Ang II for longer periods. These observations are is in agreement with the earlier data in other systems (Ullian and Linas, 1990; Hein et al., 1997).

In summary, present studies provide significant insights into the mechanism for the bimodal effect of Ang II in the smooth muscle. The contractile effect of Ang II occurs by the activation of $AT_1$-R (situated mostly in the PM) and the relaxation component via $AT_2$-R (situated normally in the cytosol). Higher concentrations of Ang II cause internalization of the $AT_1$-R to the cytosol and externalization of $AT_2$-R to the PM. This process exposes $AT_2$-R for the activation. However, the molecular events leading up to the above pattern of movement of Ang II receptors remain to be determined.

## References

Battish R, Cao GY, Lynn RB, Chakder S, and Rattan S (2000) Heme oxygenase-2 distribution in anorectum: colocalization with neuronal nitric oxide synthase. *Am J Physiol Gastrointest Liver Physiol* **278**:G148-G155.

Cao W, Harnett KM, Behar J, and Biancani P (2002) $PGF_{2\alpha}$-induced contraction of cat esophageal and lower esophageal sphincter circular smooth muscle. *Am J Physiol Gastrointest Liver Physiol* **283**:G282-G291.

Chiba Y, Uchida T, Sakai S, Oku T, Itoh S, Tsuji T, and Misawa M (2004) Acetylcholine-induced translocation of Rhoa in freshly isolated single smooth muscle cells of rat bronchi. *J Pharmacol Sci* **95**:479-482.

Chomczynski P and Sacchi N (1987) Single step method of RNA isolation by acid guanidinium thiocyanate-phenol-chloroform extraction. *Anal Biochem* **162**:156-159.

De Gasparo M, Catt KJ, Inagami T, Wright JW, and Unger T (2000) International union of pharmacology. XXIII. The angiotensin II receptors. *Pharmacol Rev* **52**:415-472.

De Godoy MAF and De Oliveira AM (2002) Cross-talk between $AT_1$ and $AT_2$ angiotensin receptors in rat anococcygeus smooth muscle. *J Pharmacol Exp Ther* **303**:333-339.

De Godoy MAF, De Oliveira AM, and Rattan S (2004a) Angiotensin II-induced relaxation of of anococcygeus smooth muscle via desensitization of $AT_1$ receptor, and activation of $AT_2$ receptor associated with nitric-oxide synthase pathway. *J Pharmacol Exp Ther* **311**:394-401.

De Godoy MAF, Dunn SR, and Rattan S (2004b) Evidence for the role of angiotensin II biosynthesis in the rat internal anal sphincter tone. *Gastroenterology* **127**:127-138.

De Godoy MAF and Rattan S (2005) Autocrine regulation of internal anal sphincter tone by renin-angiotensin system: comparison with phasic smooth muscle. *Am J Physiol Gastrointest Liver Physiol* **289**:G1164-G1175.

Fukada SY, Tirapelli CR, De Godoy MAF, and De Oliveira AM (2005) Mechanisms underlying the endothelium-independent relaxation induced by angiotensin II in rat aorta. *J Cardiovasc Pharmacol* **45**:136-143.

Hein L, Meinel L, Pratt MM, Dzau VJ, and Brian KK (1997) Intracellular trafficking of angiotensin II and its $AT_1$ and $AT_2$ receptors: evidence for selective sorting of receptor and ligand. *Mol Endocrinol* **11**:1266-1277.

Huang J, Zhou H, Mahavadi S, Sriwai W, Lyall V, and Murthy KS (2005) Signaling pathways mediating gastrointestinal smooth muscle contraction and $MLC_{20}$ phosphorylation by motilin receptors. *Am J Physiol Gastrointest Liver Physiol* **288**:G23-G31.

Huang Z, Bambino T, Chen Y, Lameh J, and Nissenson RA (1999) Role of signal transduction in internalization of the G protein-coupled receptor for parathyroid hormone (PTH) and PTH-related protein. *Endocrinology* **140**:1294-1300.

Kim J, Ahn S, Ren XR, Whalen EJ, Reiter E, Wei H, and Lefkowitz RJ (2005) Functional antagonism of different G protein-coupled receptor kinases for beta-arrestin-mediated angiotensin II receptor signaling. *Proc Natl Acad Sci USA* **102**:1442-1447.

Lazard D, Villageois P, Briend-Sutren MM, Cavaillé F, Bottari S, Strosberg AD, and Nahmias C (1994) Characterization of a membrane glycoprotein having pharmacological and biochemical properties of an $AT_2$ angiotensin II receptor from human myometrium . *Eur J Biochem* **220**:919-926.

Lowry OH, Rosebrough NJ, Farr AL, and Randall RJ (1951) Protein measurement with the Folin phenol reagent. *J Biol Chem* **193**:265-275.

Olivares-Reyes JA, Smith RD, Hunyady L, Shah BH, and Catt KJ (2001) Agonist-induced signaling desensitization, and internalization of phosphorylation-deficient $AT_{1A}$ angiotensin receptor. *J Biol Chem* **276**:37761-37768.

Rattan S and Chakder S (1992) Role of nitric oxide as a mediator of internal anal sphincter relaxation. *Am J Physiol Gastrointest Liver Physiol* **262**:G107-G112.

Rattan S, Fan Y-P, and Puri RN (2002) Comparison of angiotensin II (Ang II) effects in the internal anal sphincter (IAS) and lower esophageal sphincter smooth muscles. *Life Sci* **70**:2147-2164.

Rockman HA, Choi DJRNU, Akhter SA, Lefkowitz RJ, and Koch WJ (1996) Receptor-specific in vivo desensitization by the G protein-coupled receptor kinase-5 in transgenic mice. *Proc Natl Acad Sci USA* **93**:9954-9959.

Siragy HM, De Gasparo M, and Carey RM (2000) Angiotensin type 2 receptor mediates valsartan-induced hypotension in conscious rats. *Hypertension* **35**:1074-1077.

Turu G, Szidonya L, Gaborik Z, Buday L, Spat A, Clark AJ, and Hunyady L (2006) Differential β-arrestin binding of $AT_1$ and $AT_2$ receptors. *FEBS Lett* **580**:41-45.

Ullian ME and Linas SL (1990) Angiotensin II surface receptor coupling to inositol trisphosphate formation in vascular smooth muscle cells. *J Biol Chem* **265**:195-200.

Wu L, Iwai M, Nakagami H, Li Z, Chen R, Suzuki J, Akishita M, De Gasparo M, and Horiuchi M (2001) Roles of angiotensin II type 2 receptor stimulation associated with selective angiotensin II type 1 receptor blockade with valsartan in the improvement of inflammation-induced vascular injury. *Circulation* **104**:2716-2721.

Yang J, Clark JWJr, Bryan RM, and Robertson C (2003) The myogenic response in isolated rat cerebrovascular arteries: smooth muscle cell model. *Med Enz Phys* **25**:691-709.

## Footnotes

The studies were supported by National Institutes of Diabetes and Digestive and Kidney Diseases Grant DK-35385 and an institutional grant from Thomas Jefferson University, Philadelphia, PA.

**Name and address to receive reprint requests:**

Dr. Satish Rattan, Jefferson Medical College, Thomas Jefferson University, 1025 Walnut Street, Room # 901 College; Philadelphia, PA 19107

Tel # (215) 955-5614; Fax # (215) 503-3771; Email: Satish.Rattan@Jefferson.edu

## Figure Legends

**Fig. 1:** Bimodal effect of Ang II on rat internal anal sphincter (IAS) smooth muscle cells (SMC). The contraction phase is inhibited by losartan ($AT_1$-R antagonist) while PD123,319 ($AT_2$-R antagonist) has no significant effect. Conversely, PD123,319 but not losartan inhibits the relaxation component. Data represent the mean ± SEM, n = 3; One-way ANOVA; *; $p < 0.05$ compared with 100 nM)

**Fig. 2:** Time course for the $AT_1$-R internalization (A) and $AT_2$-R externalization (B) in the presence of 10 μM Ang II using Sulfo-NHS-SS-biotinylation of the cells. This was followed by lysis, protein extraction, and isolation of biotinylated proteins using a streptavidin-gel matrix. Specific IR for $AT_1$-R and $AT_2$-R at the cell surface was determined by Western blot. Ang II induces a decrease in $AT_1$-R and an increase in the $AT_2$-R density at the cell surface in a time-dependent manner which plateaus at 10 min. Data are expressed as % maximal change as mean ± SEM, n = 3. The significance of the differences at various time points for $AT_1$- or $AT_2$-R was determined in comparison with their respective basal values at 0 min (one way ANOVA: *; $p < 0.05$). Not shown, bethanechol (100 μM), causes no significant change in the cell surface population of either the $AT_1$- or $AT_2$-R.

**Fig. 3:** Confocal images of the SMC specifically stained for $AT_1$-R and observed under a Texas red filter (**A**). Note higher density of $AT_1$-R on the plasma membrane (PM) in the basal state (**a**). Incubation with 100 nM (**b**) and 10 μM (**c**) Ang II induces receptor internalization to the cytosol. Losartan causes an increase in the $AT_1$-R density in the PM of the non stimulated cells (**d**) but inhibits the receptor internalization by Ang II (**e** and **f**). PD123,319 on the other hand has no effect under any of the conditions tested (**g**, **h**, and **i**). The solid arrows indicate receptors on the PM, and dashed arrows indicate the receptors in the cytosolic pool. Change in cellular distribution of $AT_1$-R in freshly isolated rat IAS SMC (**B**). The graph shows the peripheral to cytosolic ratio (mean ± S.E.M) of $AT_1$-R in IAS cells. Ang II-induced receptor trafficking from PM to cytosol is inhibited by losartan. Statistical significance was calculated by ANOVA (*; $p < 0.05$) compared with basal.

**Fig. 4:** Confocal images of the SMC specifically stained for $AT_2$-R and observed under a FITC filter (**A**). Note higher intensity of $AT_2$-R in the cytosolic pool in the basal state (**a**). Incubation with 100 nM (**b**) and 10 µM (**c**) Ang II induces receptor migration from the cytosol. Incubation with losartan does not produce any effect in the basal state (**d**) but does inhibit the receptor migration from the cytosol following Ang II (**e** and **f**). PD123,319, on the other hand, has no effect under any of the conditions tested (**g**, **h**, **i**). The solid arrows indicate receptors on the PM, and dashed arrows in the cytosolic pool. Cellular distribution of $AT_2$-R in the IAS SMC (**B**). The graph shows the peripheral to cytosolic ratio (mean ± S.E.M ) of $AT_2$-R in IAS cells. Ang II induces significant receptor trafficking from cytosol to PM which is inhibited significantly by losartan. (ANOVA; *; $p < 0.05$).

**Fig. 5:** Effects of different concentrations of Ang II on the cytosolic and particulate $AT_1$-R (**A**) and $AT_2$-Rs (**B**) in the IAS SMC. Note predominance of $AT_1$-R in the particulate fraction in the basal state, and their migration to the cytosol upon exposure to high concentrations of Ang II. On the other hand, $AT_2$-R are present predominantly in the cytosol and migrate in the opposite direction towards the PM (panel **B**). This migration of $AT_2$-R occurs specifically in the form of $AT_2$-R homodimer as shown in panel B. Data represent the mean ± SEM; n = 3. Statistical significance was calculated by ANOVA (*; $p < 0.05$).

**Fig. 6:** Exposure of the SMC with 10 µM Ang II (30 min) caused no significant difference in the total cellular contents of $AT_1$-R (**A**) and $AT_2$-R (**B**) ($p > 0.05$; n = 3). Data are expressed as mean ± SEM.

**Fig. 7:** Exposure of the SMC with 10 µM Ang II (30 min) caused no significant change in the PCR products encoding $AT_1$-R (**A**) and $AT_2$-R (**B**) ($p > 0.05$; n = 3). Data are expressed as mean ± SEM.

JPET Fast Forward. Published on September 19, 2006 as DOI: 10.1124/jpet.106.108084
This article has not been copyedited and formatted. The final version may differ from this version.



**TABLE 1**

Primers used in RT-PCRs for amplification of mRNA encoding $AT_1$-R, $AT_2$-R, and β-actin in IAS smooth muscle cells

| Primer | Strand | Sequence (5' – 3') | Accession No. |
|---|---|---|---|
| **$AT_1$** | Forward | CTACAGCATCATCTTTGTGGTGGGA | NM_030985 |
| | Reverse | CGTAGACAGGCTTGAGTGGGACTT | |
| **$AT_2$** | Forward | TCTCAACGCAACTGGCACCAATGAG | NM_012494 |
| | Reverse | CTCTCTCTTGCCTTGGAGCCAAGTA | |
| **β-actin** | Forward | TGTTTGAGACCTTCAACACCCC | NM_007393 |
| | Reverse | ACGTCACACTCCATGATGGAA | |

**TABLE 2**

Values of $E_{max}$ and $pD_2$ for the contraction phase of Ang II in the SMC Isolated from IAS

| **Treatment** | **$E_{max}$[a] (%)** | **$pD_2$[b]** |
|---|---|---|
| Control | 22.5 ± 2.2 | 7.8 ± 0.2 |
| Losartan (0.1 μM) | 10.6 ± 1.8[c] | 7.0 ± 0.1[c] |
| PD123,319 (0.1 μM) | 19.8 ± 2.3 | 7.9 ± 0.3 |

[a]$E_{max}$ is defined as the maximal contraction by Ang II. Data represent the mean ± SEM of 4 to 7 independent determinations.

[b]$pD_2$ is the -log $EC_{50}$ (concentration of the agonist that produces a 50% contraction of smooth muscle).

[c]$p < 0.05$ compared with the respective control (1-way analysis of variance).

JPET Fast Forward. Published on September 19, 2006 as DOI: 10.1124/jpet.106.108084
This article has not been copyedited and formatted. The final version may differ from this version.

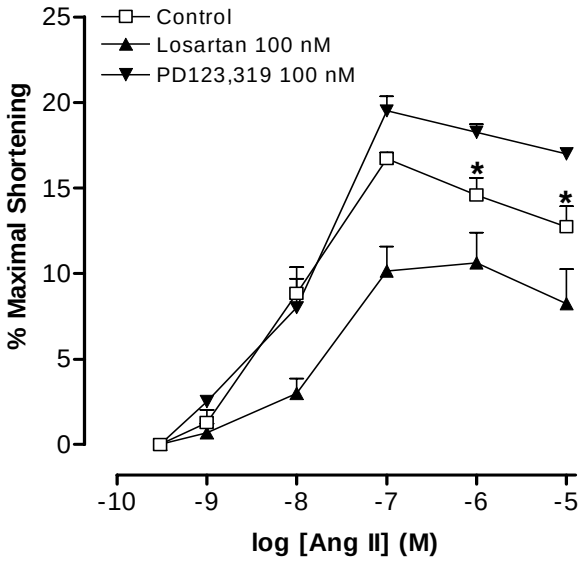


**Figure 1**

JPET Fast Forward. Published on September 19, 2006 as DOI: 10.1124/jpet.106.108084
This article has not been copyedited and formatted. The final version may differ from this version.

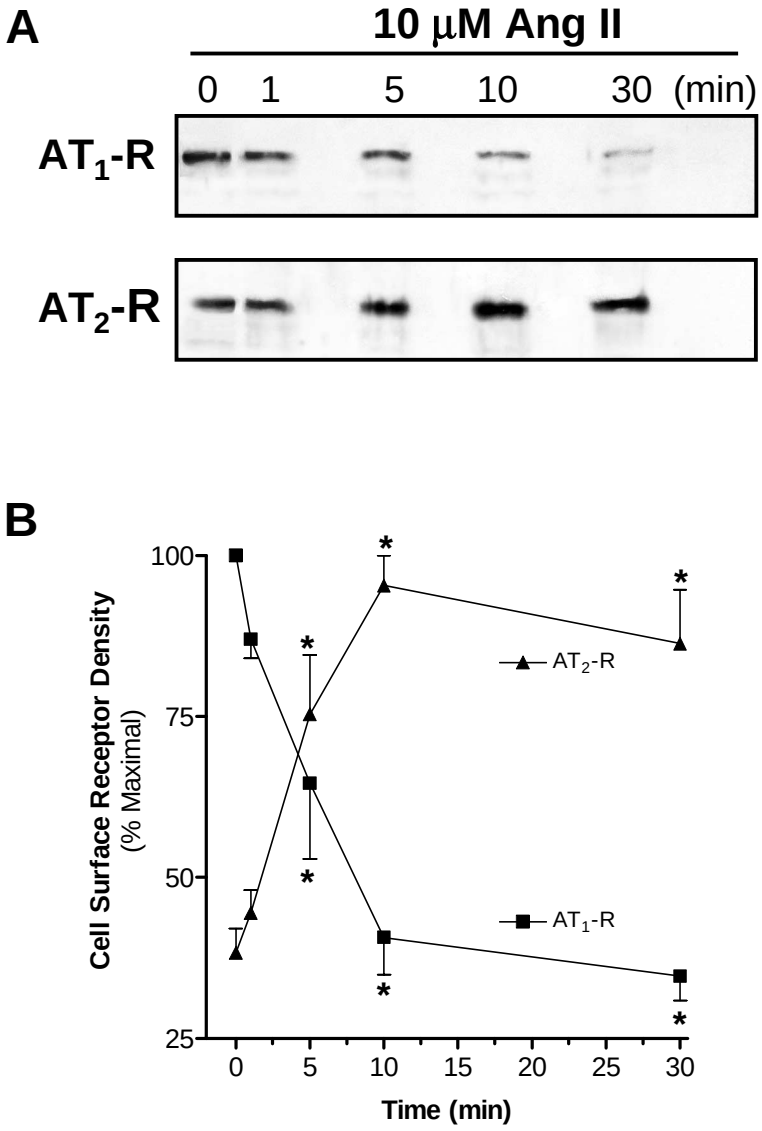


**Figure 2**

JPET Fast Forward. Published on September 19, 2006 as DOI: 10.1124/jpet.106.108084
This article has not been copyedited and formatted. The final version may differ from this version.

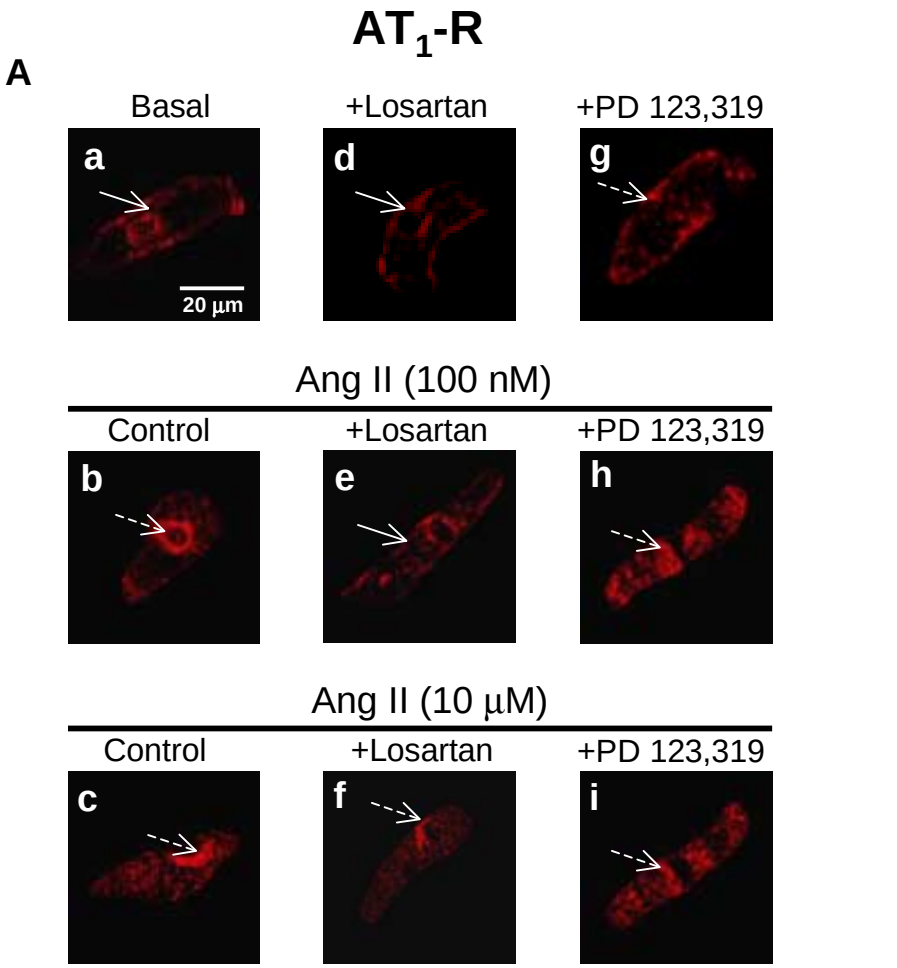


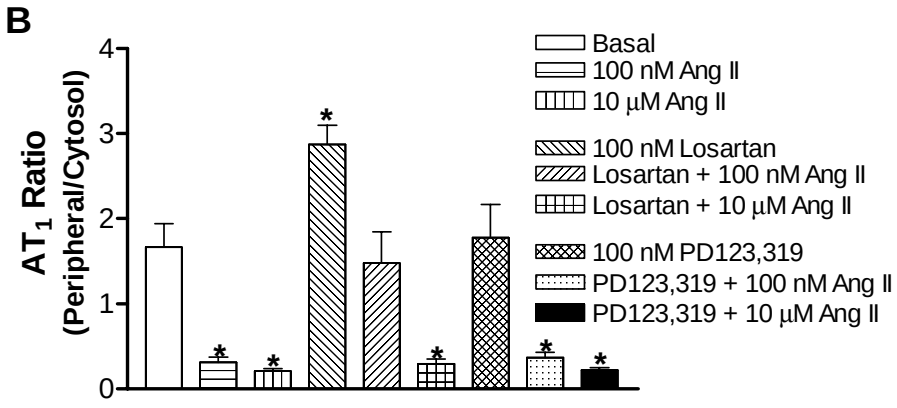


Figure 3

JPET Fast Forward. Published on September 19, 2006 as DOI: 10.1124/jpet.106.108084
This article has not been copyedited and formatted. The final version may differ from this version.

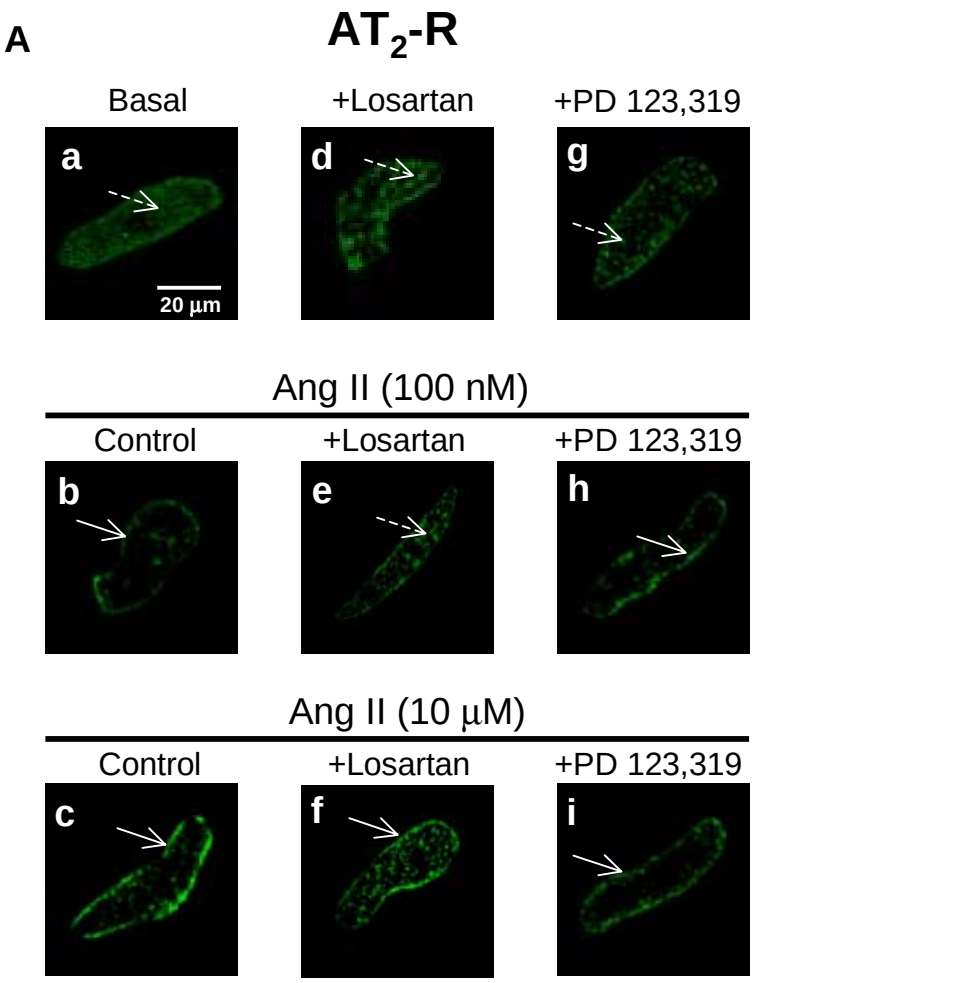


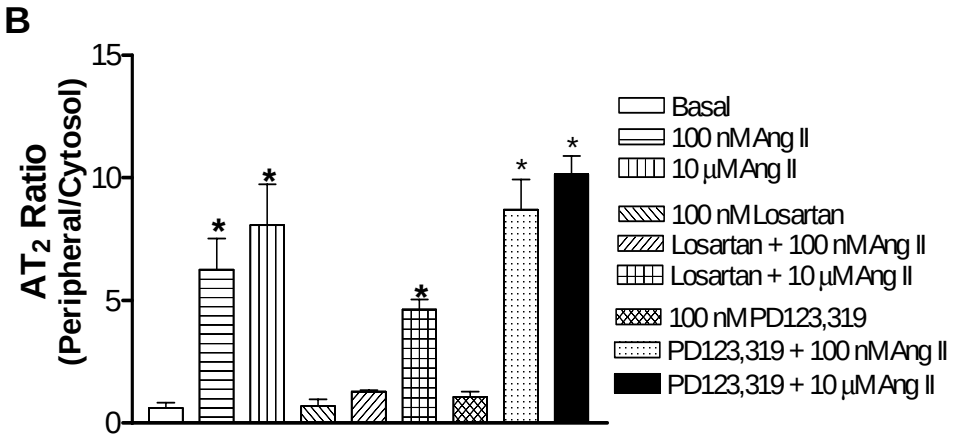


Figure 4

JPET Fast Forward. Published on September 19, 2006 as DOI: 10.1124/jpet.106.108084
This article has not been copyedited and formatted. The final version may differ from this version.

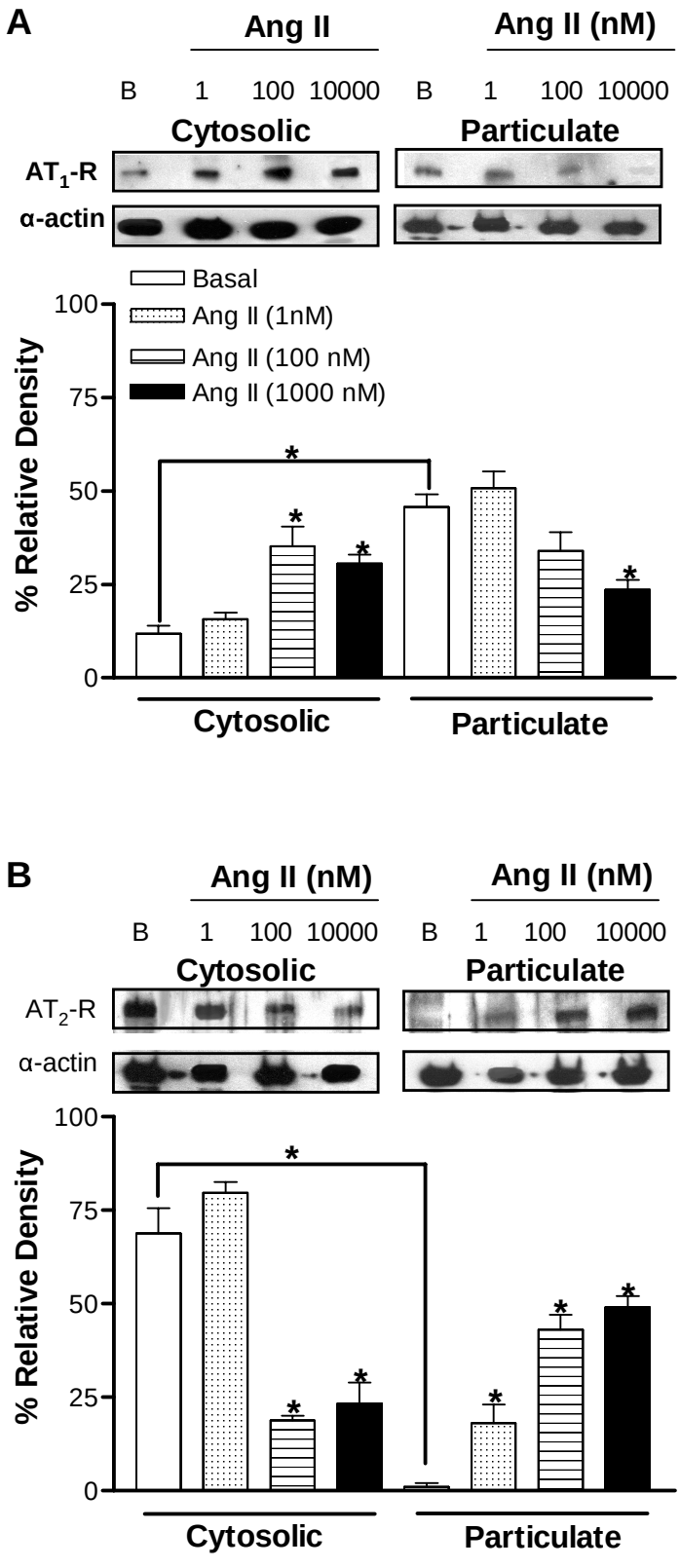


**Figure 5**

JPET Fast Forward. Published on September 19, 2006 as DOI: 10.1124/jpet.106.108084
This article has not been copyedited and formatted. The final version may differ from this version.

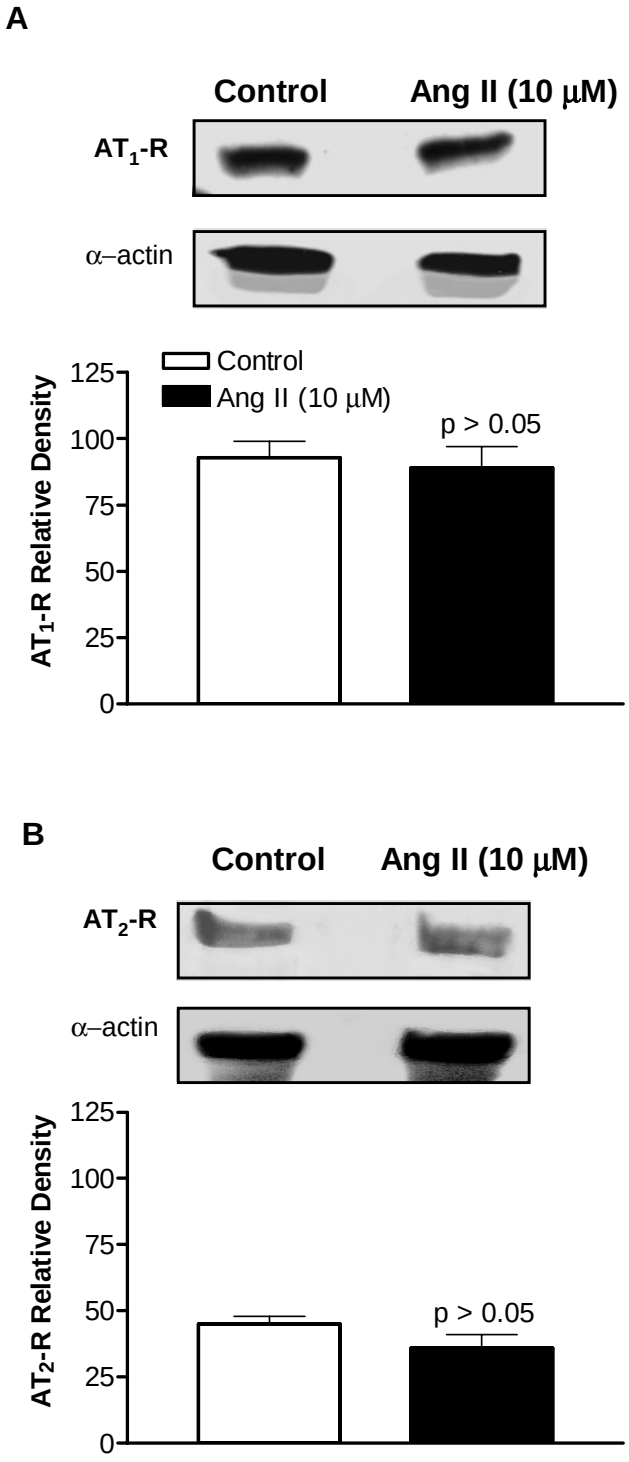


**Figure 6**

JPET Fast Forward. Published on September 19, 2006 as DOI: 10.1124/jpet.106.108084
This article has not been copyedited and formatted. The final version may differ from this version.

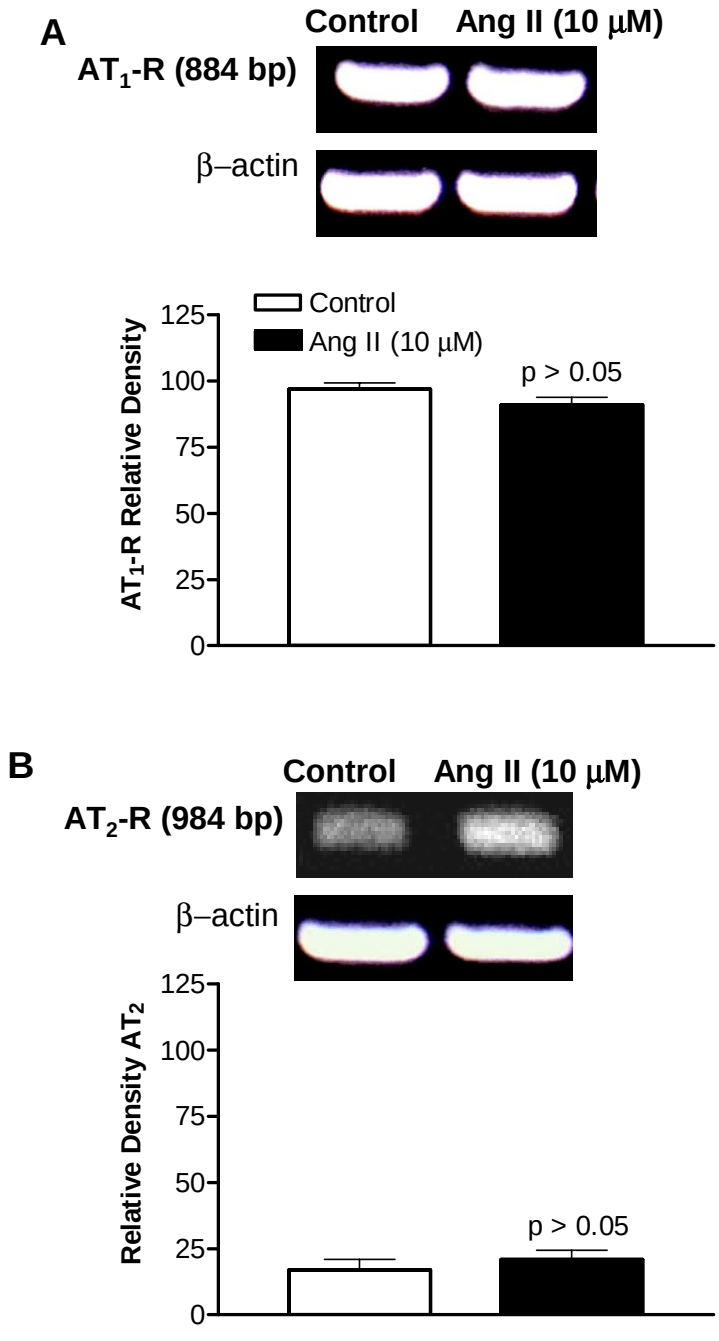


**Figure 7**